Slot Number Thermal Effects on Electrical Machines

Fengyu Zhang, David Gerada, Zeyuan Xu, Xiaochen Zhang, Chris Tighe, He Zhang, Wei Hua, Chris Gerada

***Abstract*-- While electrical machine designers typically go to great lengths to choose the optimal number of stator slots based on the electromagnetic performance, often the thermal aspects of this selection are overlooked. This paper investigates the multi-domain impacts related to the slot number selection, combining both the electromagnetic and thermal aspects. Taking an existing 42-kW 4-pole, 12-slot electrical machine with Halbach-array surface-PM rotor, used within a more-electric marine engine as a case study, performance aspects of the machine with different slot numbers are investigated. The impact of slot number is compared considering the losses, output torque and its quality, as well as the peak temperature. Experimental tests are performed, verifying significant temperature reductions and performance entitlements when the optimal stator slot number from thermal point of view is selected. Finally general guidelines on slot number selection for temperature reduction are provided.**

***Index Terms*--Thermal effects, slot number, multi-domain analysis, power density.**

I. Introduction

With the globally stringent emissions policies, increased electrification at an unprecedented rate is underway for various transportation application areas, be it for marine, aerospace, rail, or road vehicles. Different application areas have different performance metrics for electrical machines. For example for the more-electric/hybrid/electric aircraft, the power to mass ratio [kW/kg] is the key figure of merit, with outstanding values, in excess of 6kW/kg reported recently [1]. In the automotive domain, packaging [kW/L] is very important, as is cost reduction, while for marine applications where space and mass are less of an issue, high efficiencies with good cost-performance [$/kW] are sought [2]. For all the aforementioned important key performance metrics, the thermal management and its enhancement are key in improving the performance metrics beyond the current state of the art, and help increase the market proliferation of electrified technologies [1, 3-5].

This work was supported by the China MoST project under Grant 2018B10002, 2018B10001 and 2018B10082. Paper no. TEC-00820-2019. (*Corresponding author: David Gerada*)

F. Zhang, D. Gerada, Z. Xu, and C. Gerada are with University of Nottingham, Nottingham, NG7 2RD, UK (email: Fengyu.zhang@nottingham.ac.uk; David.Gerada@nottingham.ac.uk, Zeyuan.Xu@nottingham.ac.uk, Chris.Gerada@nottingham.ac.uk).

X. Zhang and H. Zhang are with the Key Laboratory of More Electric Aircraft Technology of Zhejiang Province, University of Nottingham Ningbo China, Ningbo 315100, China (email: Xiaochen.zhang@nottingham.edu.cn; He.Zhang@nottingham.edu.cn)

C. Tighe is with Electrical Cooling Solutions Ltd, Nottingham, NG7 2TU, UK (email: chris.tighe@electricalcoolingsolutions.com).

W. Hua is with the School of Electrical Engineering, Southeast University, Nanjing, China (email: huawei1978@seu.edu.cn).

Thermal management in electrical machines combines two important main aspects: heat dissipation and heat generation. As for heat dissipation, conventional cooling methods applied in electrical machines include water channel design, housing fins, and shaft-mounted fans [6]. Water-jacket cooling [7], compared to the forced cooling methodologies [8], is a more effective way to remove heat generated inside the motor and is presently the mainstream way to cool automotive traction machines, as well as being reported for other applications where robustness is required such as in marine generators [3].

For water-jacket cooled electrical machines, improvement of the heat transfer path inside the stator slot holds the largest potential to reduce peak temperatures due to the low equivalent thermal conductivity inside the slot [9]. Using an impregnation resin with a higher thermal conductivity is a direct way to increase the slot heat transfer ability. Three impregnation resin candidates, including varnish, Epoxylite and a silicone-based thermally conductive material SbTCM, are discussed and experimentally tested on identical induction machines [10]. Significant temperature reduction is observed in electrical machines using impregnation material with higher thermal conductivities. However, from the authors' experience, the higher the impregnation material's thermal conductivity, the higher its cost. Furthermore, higher thermal conductivity resins tend to have lower dielectric strengths [6]. Back-iron extension, whereby part of the back-iron is extended into the slot, proposed in [11], can achieve around 25% temperature reduction and does not have any associated cost-premium. However it is mainly applicable for concentrated-wound machines. Slot water jacket cooling provides another efficient way of winding cooling [12]. A heat exchanger inside the slot is presented in [13], shortening the heat transfer path between the heat sources and the fluid with a reported sustained current density of over 24A/mm^2. As with the case of the water pipes, reliable sealing is needed, and it is more suitable for electrical machines with concentrated windings.

In [4], a novel 'T'-shaped copper heat path is inserted from the centre of the slot to the bottom of the slot for a low frequency machine, where the large base provides a large contact area to the stator lamination. Having high thermal conductivity, the copper largely shortens the heat transfer path between the slot and the coolant, resulting in a 40% temperature reduction for the same current loading. However, eddy losses caused within the copper plate would nullify the thermal benefits in higher frequency electrical machines.

Parallel and trapezoidal stator slot shapes are compared with respect to loss distribution and thermal benefits in [14]. It is concluded that with a parallel sided slot design, a 37 °C winding

temperature reduction is achieved, or alternatively an 11% increase in the torque production at the intended machine operation point is achieved. It is worth noting that this methodology is only applied to open modular stator windings [14]. Two factors regarding slot shape and slot size are researched in [15] to investigate the slot geometry thermal effects on the hardware exemplars, with equivalent thermal resistance between the winding and the coolant derived from DC power tests. The equivalent thermal resistance between the hot spot in the slot and the coolant is made up of several separate resistive components, which include resistances passing through different materials, such as the wire enamel, slot impregnation resin, air-pockets, slot liner, stator lamination, contact resistance, water jacket and fluids. It is concluded in [9] that the radial slot thermal conductivity contributes most to the total series resistances. Therefore, for electrical machines having the same size, the slot radial resistance is quite sensitive to the slot number. Higher slot number provides increased dissipation contact area from the slot to the coolant, while it also means reduced volume available for the armature windings.

The number of slots per pole per phase ‘q’ is a key electrical machine designer’s design variable, typically optimising its value for specific electromagnetic aspects such as torque quality and inductance tailoring, while its effects on the thermal behavior of the electrical machine are often overlooked. This paper adopts a multi-domain approach to investigate the thermal aspects related to the slot number selection, in conjunction with the electromagnetic aspects such as the output torque and its quality, with the analysis conducted validated by experimental tests.

Segments (motorettes) are a time and cost-effective way to validate the conducted analysis, allowing for adequate variants to be manufactured and compared [16, 17]. Winding losses are typically the main source of power losses and a power-density bottleneck within high performance PM machines, which result into high operating winding temperatures. Careful thermocouple placement within the segments is thus very important [18]. In this paper, segments corresponding to machines with different slot number are used to validate the thermal effects’ analysis. This paper is organized as follows: section II investigates the multi-domain impacts for four electrical machines with different stator slot number from both the electromagnetic and thermal perspectives. In section III, experimental tests are performed on prototyped sections, in order to validate the analysis results. Finally, conclusions and design recommendations based on this research are summarized in section IV.

II. MACHINES WITH DIFFERENT SLOT NUMBER

In water-jacket-cooled machines, most of the heat generated in the slot is dissipated to the coolant through the stator slot, slot wall and back-iron. The slot consists of multiple materials, including the copper wire itself, where the heat is generated. The wire is often coated with insulating enamel, resin which fills the gaps between strands and helps stiffen the windings, and the slot-liner which provides the phase electrical insulation. Given the low slot effective circumferential thermal conductivity, therefore, the radial slot thermal resistance is significant in determining the hot spot temperature in the slot. The hot spot is usually located in the centre of the slot, furthest away from the iron. For the same stator inner diameter and outer diameter, increasing the slot number reduces the slot width and hence reduces the distance between the centre of the slot and the tooth. On the other hand from a thermal perspective, with increased slot number, the amount of slot liner also increases, hence reducing the available space for copper. Meanwhile, from the electromagnetic side, different slot numbers have sensitive effects on machine performances.

Taking an existing 42 kW, 4-pole, 12-slot (i.e. slot per pole per phase 'q'=1) constant speed electrical machine used within a marine engine waste heat recovery system as a case study, shown in Fig. 1, the thermal effects of the original motor and the proposed motors with different slot numbers (24-slot, 36-slot and 84-slot) are studied in this section, alongside the electromagnetic aspects.

Fig. 1. Original 42kW 4-pole electrical machine

In all the motors considered within the study, the Halbach-array surface-PM rotor is kept the same. The total slot area is also kept constant, which includes the winding area, the slot liner area, and the wedge area. The ratio of total copper area to total slot area is named as the ‘copper fill factor’ in this paper. To generate the copper fill factor, the ratio of copper area to the available winding area (slot area minus slot-liner area) is kept constant. As the slot number increases, the amount of slot liner increases, which results in less available winding area and hence copper fill factor reduction, as shown in Fig. 2. The copper fill factor decreases almost linearly from 0.4535 in the original 12-slot motor, down to 0.3712 for the 84-slot motor. In this section, firstly, the electromagnetic aspects of all the considered motors are investigated. Thermal modelling is then presented in the second part, with machine performances compared for the same output torque. Thermal results are presented in the last part of this section, as an output of this study, in order to understand better the trade-offs in hand.

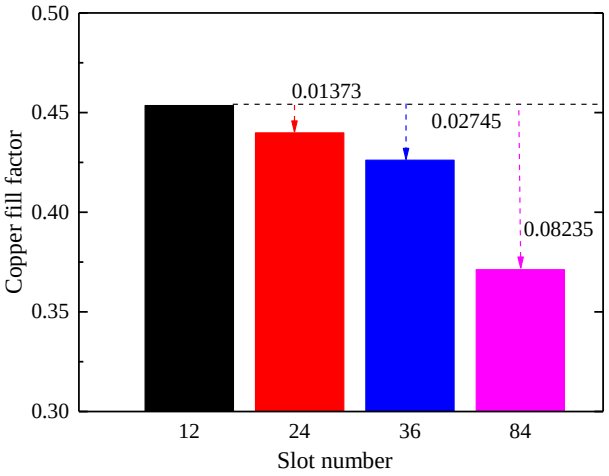

Fig. 2. Copper fill factor variation with slot number

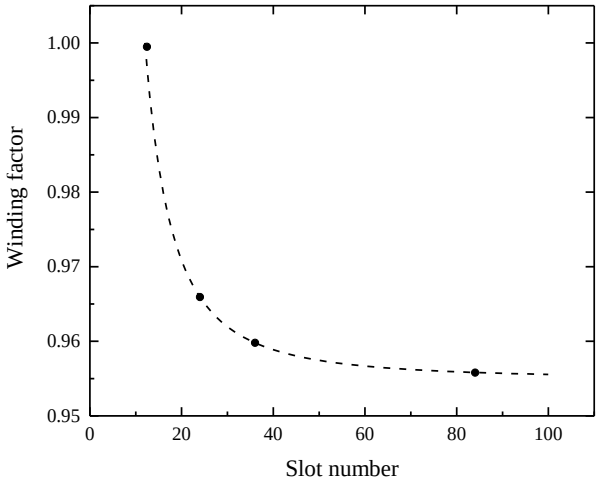

Fig. 3. Winding factor variation with slot number

A. Electromagnetic aspects

The winding factor 'k_w' is an important parameter in the motor design process, and high values are sought to maximise the efficiency of the winding design. It is calculated from (1),

$$k_w = k_p \times k_d \quad (1)$$

where 'k_p' is the pitch factor, which depends on the slot pitch and pole pitch [15]. A single layer fully-pitched winding is adopted in this study, and hence 'k_p' is always equal to 1. The winding of AC machines is distributed in several slots per pole pitch. A phase consists of a number of coils connected in series and/or parallel. There is phase displacement among the electromotive forces (emfs) generated in various coils. As a result, the resultant emf per phase is the phasor sum of various emfs generated in the coils of that phase. Hence the resultant electromotive force (emf) is always less than the arithmetic sum of the separate emfs. The ratio of resultant phase emf to the arithmetic sum of separate emfs of coils of a phase is called the distribution factor, 'k_d', which is expressed as:

$$k_d = \frac{\sin(q\alpha/2)}{q\sin(\alpha/2)} \quad (2)$$

where 'q' is the number of stator slots per pole per phase and 'α' is the slot pitch angle.

The reduction of the winding factor with slot number is plotted in Fig. 3, according to which, the winding factor decreases by down to 4.42% from the original motor to the 84-slot motor.

The winding factor is not the only parameter which needs careful consideration. The inductance also changes with the slot number, with the slot leakage inductance being approximately inversely proportional to the slot number [18]. Finite Element Analysis (FEA) is used to analyse the nonlinear electromagnetic effects of the motors with the proposed slot numbers, outputs of which, including flux density, output torque, and torque ripple are assessed. Fig. 4. shows the slot configurations and FEA-computed flux-density plots for the machine variations of this study.

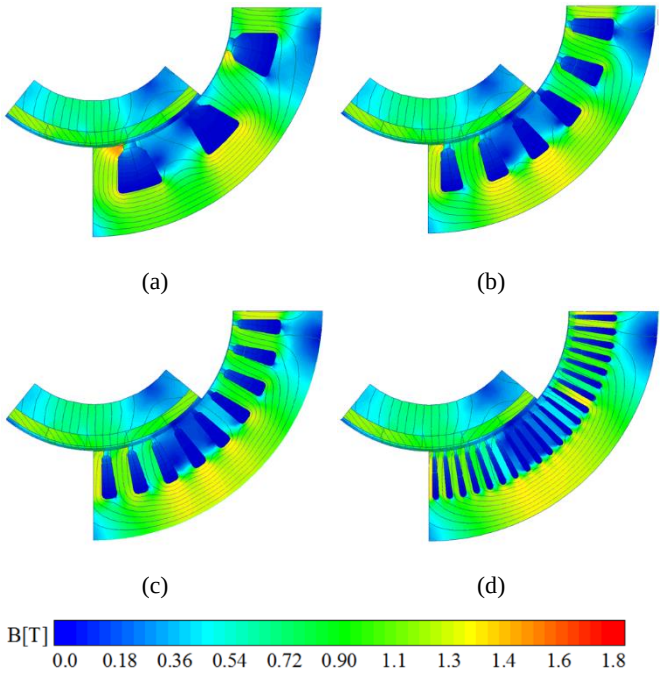

Fig. 4. Flux density plot for each machine (a) original 12-slot motor; (b) 24-slot motor; (c) 36-slot motor; (d) 84-slot motor

Due to the combined effects of reduced winding factor on one hand and reduced slot leakage on the other hand, from Fig. 5, it can be observed that the overall output torque reduces with the increasing slot number, when the motors are fed with the same current. A significant torque reduction by down to 2.07N·m (2.4%) is shown when the slot number is increased from 12 to 24. This percentage reduction roughly corresponds to the reduction in the winding factor, indicating that for this case the reduction in winding factor effect is predominant over any gains in reduced slot leakage when doubling the slot number. When the slot number increases from 36 to 84, no significant further torque reduction is observed from Fig. 5, again following the trend of the winding factor of Fig. 3.

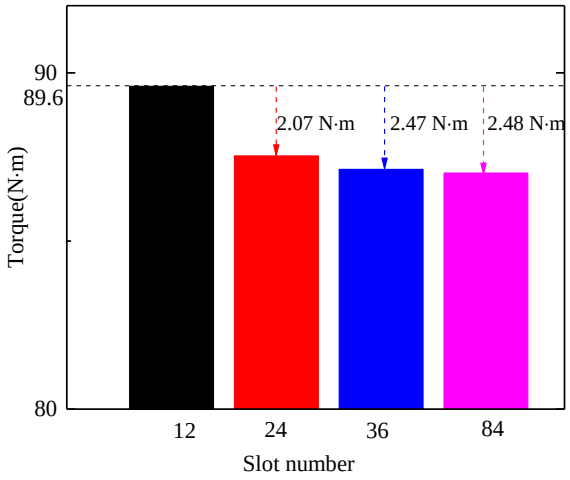

Fig. 5. Torque comparison with different slot number

Based on the foregoing analysis, input current is then increased with the slot number in order to maintain the same output torque as in the original 12-slot motor. The current required is indicated in Fig. 6. The current increase shows similar tendency to the torque reduction in Fig. 5, since the machine is not highly saturated. For the 24-slot motor, a current increase of 1.8A (2.46%) is demanded to obtain the same output torque of 89.6 N·m as with the original motor, as shown in Fig. 6, while it is 2A (2.74%), 2.11A (2.89%), respectively for the 36-slot and 84-slot motors. The increased current contributes to higher copper and iron losses, influencing the thermal conditions of the electrical machines.

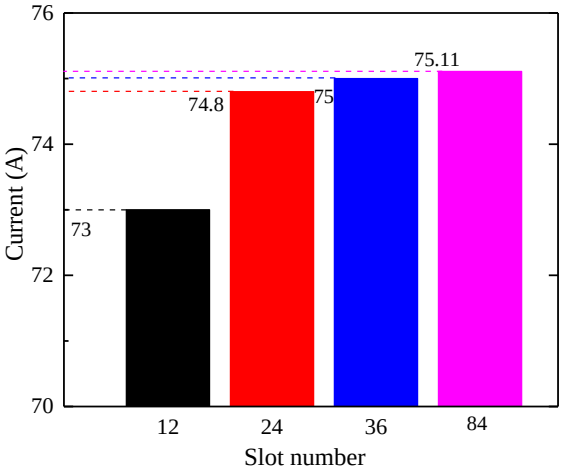

Fig. 6. Current requirement for the same output torque

Torque ripple is another factor that needs consideration when different slot numbers are used. With the same rotor design (Halbach SPM, as shown in Fig. 4), the torque ripple variation with slot number is shown in Fig. 7. The torque ripple generated with the 24-slot motor remains almost constant as with the original motor, while for the 36-slot and 84-slot motors, torque ripple gets markedly improved from 15% down to below 3%.

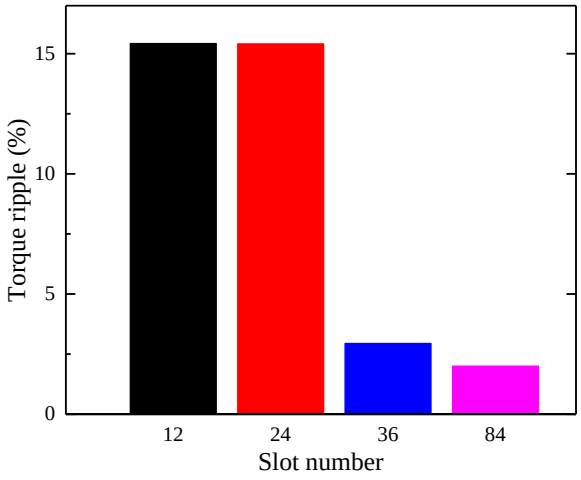

Fig. 7. Torque ripple comparison for different slot numbers

Losses generated in the motor play a vitally important role from both electromagnetic and thermal perspectives, and together with the thermal management are the main factors determining the limits of performance metrics.

Losses for each machine variant considered within this paper are composed primarily of stator copper losses and stator iron losses. Only DC copper losses are considered in this section as the machine is operating at a low frequency and AC losses are negligible compared to DC losses. The copper losses are calculated with formulae (2) and (3).

$$P_{cu} = 3{I_{ph}}^2 R_{ph} \tag{2}$$

where 'I_{ph}' and 'R_{ph}' are the phase current and phase electrical resistance of the winding respectively. It is worth noting that the electrical resistance 'R_{ph}' is coupled with the output winding temperature 'T_{ave}' from the thermal modelling results in section IIC, as shown in formula (3).

$$R_{ph} = R_{ph0}(1 + \alpha(T_{ave} - T_0)) \tag{3}$$

In (3), R_{ph0} is the electrical resistance at a known temperature T_0 (normally 20 °C), while α is the copper wire temperature coefficient, which is 0.00404.

The copper losses are allocated between the in-slot and end-winding region based on the proportion of winding length within the core and outside respectively. Meanwhile, it is worth noting that in practice the length of mean turn might change slightly for different slot numbers due to the practical winding implementation, however this is considered constant for the purpose of this study since both the pole number and stator diameters are constant.

Iron losses 'P_{Fe}' are computed directly from 2D FEA, which uses Bertotti's formulation method, and are composed of three components: hysteresis, classical and excess loss, as described by formula (4) [19, 20]

$$P_{Fe} = k_h f B^{\alpha} + k_{eddy} f^2 B^2 + k_{exc} f^{1.5} B^{1.5} \tag{4}$$

where 'k_h', 'k_{eddy}', and 'k_{exc}' are the hysteresis, eddy current

and excess loss coefficients, respectively. Furthermore, 'f' and 'B' denote the frequency and magnetization, respectively. In this paper for the electrical steel grade considered, 'k_h'=0.02307, 'k_{eddy}'=1.141×10^{-6}, and 'k_{exc}'=0.0008532, while 'α' =1.975.

The variation of the aforesaid losses with slot number is shown in Fig. 8. Over the range of investigated slots, the magnitude of the copper losses in Fig. 8(a) increases with slot number by 30% from 1018W to 1321W for the same output torque. The increase in the winding losses are mainly due to two factors: (i) copper fill factor reduction, as shown in Fig. 2, which results in higher winding electrical resistance; and (ii) current increase required to compensate for the reduced winding factor caused by the higher slot number, as shown in Fig. 6. As the current is increased, the working flux level in the machine increases due to the stronger armature reaction field, which in turn increases the stator iron losses by up to 10.7%, from 382.5W to 422.8W across the minimum and maximum slot numbers considered in this study, as shown in Fig. 8 (b).

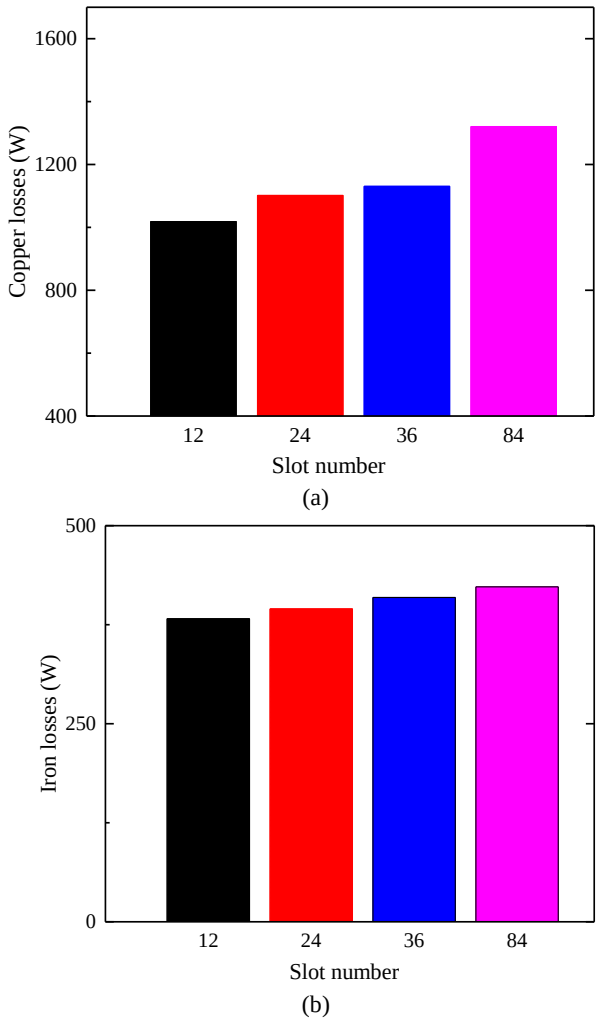

Fig. 8. Losses for motors with different slot number and same output torque (a) Copper losses; (b) iron losses

B. Thermal modelling

Lumped Parameter Thermal Network (LPTN) classifies the temperature distribution of a physical system into a topology of entities, which are linked with thermal resistances. A LPTN model is created based on the original machine topology and applied to investigate the slot number effects on machine thermal performances in this research. The process of developing such thermal network is as follows.

Half slot of the stator and corresponding part of the rotor are simulated given the motor radial geometry symmetry and periodicity. There are three corresponding repeated radial planes arranged and created longitudinally in the core to obtain the 3D detailed temperature distribution of the machine (hereafter referred to as 'axial section in core machine I-III'). Furthermore two corresponding axial end-winding sections are built to record the end-winding temperature profile for each side ('end-winding section' and 'NDE_end-winding section'). To avoid showing multiple repeating identical sections, only three axial sections are included in Fig. 9, while the 'axial section III' and 'NDE_end-winding section' thermal network are omitted in the figure.

In the radial plane, the stator back-iron, stator tooth, air-gap, rotor iron, magnet, and shaft are each represented by a single node, respectively. A 5×5 node arrangement in the half slot is generated to capture the temperature profile to a good resolution, as shown in Fig. 9. The node is located at the centre of each cell. It should be noted that five nodes between each two adjacent axial sections are plotted with '-▬-' to represent the slot axial thermal resistances. The resistances between other nodes in the slot are not shown in the same figure for the sake of clarity. Losses are considered to be distributed uniformly within one corresponding node.

The calculation of temperature is based on the heat balance equation (5) at each node 'i' which is illustrated in Fig. 9 under steady state. In (5), 'T_i' and 'q_i' are the node 'i' temperature and the associated node loss, 'T_j' is the node 'j' temperature, while 'R_{ij}' is the thermal resistance between node 'i' and node 'j'. The parameter 'n' is the total node number in Fig. 9.

$$\sum_{j\neq i}^{n} \frac{T_j - T_i}{R_{ij}} + q_i = 0 \qquad (5)$$

Only conduction and convection heat transfer are considered in this paper. Thermal conduction is the transfer of internal energy by microscopic diffusion and collisions of particles or quasi-particles within a body or between contiguous bodies [21], while convection takes places between a solid surface and a fluid when there is a temperature gradient. Convective heat transfer occurs in the modelling mainly (i) in the end-region of the motor, where the end-winding is in contact with the air; (ii) across the air-gap between the stator and rotor; (iii) in the water-jacket coolant channel within the machine aluminium housing.

The nodes displayed in Fig. 9 are linked with thermal resistances. Formulae (6) and (7) are applied in calculating the conduction and convection thermal resistance between neighbouring nodes (both radially and axially), respectively. In these formulae, 'L' in [m], is the distance between two neighbouring nodes, and 'A_{cross}' in [m^2] is the cross-sectional area that is perpendicular to the direction of heat flow between

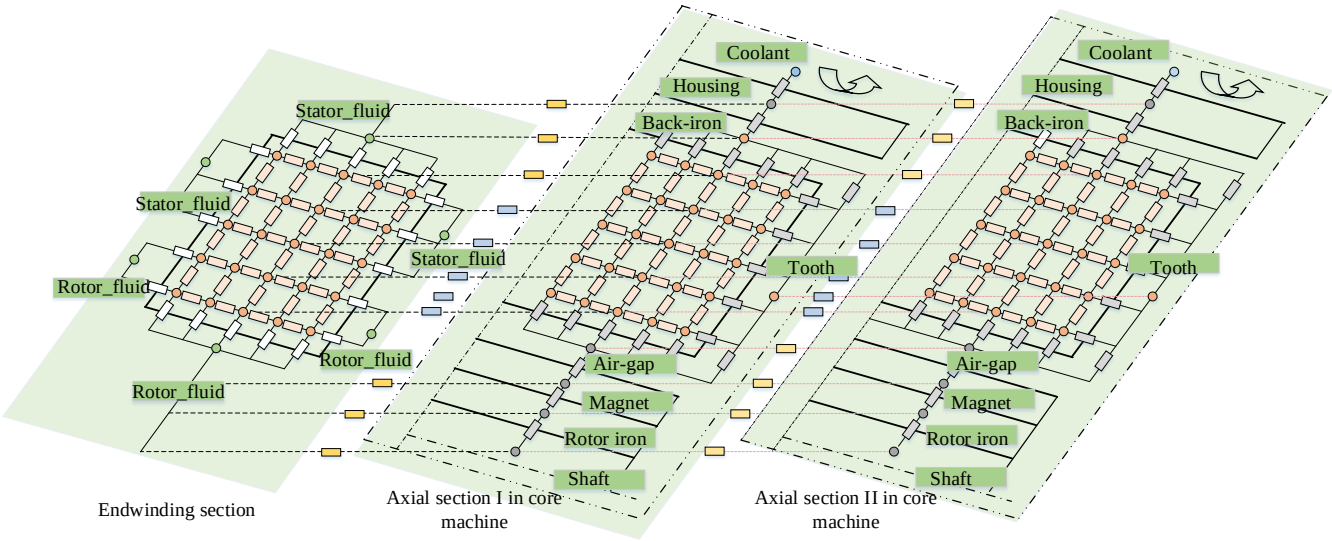

Fig. 9. 3D thermal network for the traction motor

the two nodes, while λ in [W/mK] is the effective thermal conductivity between the two nodes and is determined by the conducting material between them. Table 1 lists the main machine materials and their corresponding thermal conductivities as used within the thermal modelling. It is worth noting that the insulation system is rated to thermal class H, i.e. 180°C. Inside the slot, where multiple materials are employed, the slot effective thermal conductivity 'λ_{slot}' is used [22].

$$R_{cond} = \frac{\mathrm{L}}{\lambda A_{cross}} \tag{6}$$

$$R_{conv} = \frac{1}{hA_{sur}} \tag{7}$$

For the convection thermal resistance, 'A_{sur}' in [m^2] is the surface area of the solid in contact with the fluid around it, while 'h' in [W/m^{2}K] is the heat transfer coefficient which depends on the fluid flow near the surface. The heat transfer coefficients 'h' for the aforementioned three regions where convective heat transfer occurs are calculated using formulae (8) to (14) [23, 24].

TABLE 1
CONSTITUENT MATERIAL THERMAL CONDUCTIVITY

Item	Material	Thermal conductivity (W/mK)
Insulation (class H)	polyesterimide	0.21
Slot liner	Nomex 410	0.14
Impregnation resin	Epoxylite	0.21
Magnet	NdFeB	8.5
Stator lamination	M235-35A	29.1 (radial) 0.87 (axial)
Sleeve	Carbon fiber	0.59
Housing	Aluminum	180
Shaft	Steel 304	14.9

The heat transfer coefficient 'h' at the end-winding surface in the end-region of the motor can be estimated by an empirical formula (8) based on experimental studies [23]. The heat transfer coefficient is calculated taking into account the machine shaft speed which drives the fluid flowing around the end-winding region. Formula (8) suggests 'h' is in positive correlation with the reference velocity 'U'. With the thermal modelling in this paper, k_1=15, k_2=0.15, k_3=1. The convection heat transfer coefficient derived is around 62.5 W/(m^2·K).

$$h = k_1 \times (1 + k_2(U)^{k_3}) \tag{8}$$

Heat transfer coefficient in the air-gap mainly depends on the rotor speed and the physical air-gap length between the stator bore and the rotor outer surface. It is proposed in [23] that the heat transfer coefficient can be calculated with formulae (9) and (10),

$$Ta=Re\sqrt{a/R_r};\ \mathrm{Re} = \rho v a/\mu;\ D_e = 2a \tag{9}$$

$$h = 0.386\ \lambda\ Ta^{0.5}Pr^{0.27}/D_e \tag{10}$$

where 'Ta' is the Taylor number, 'Re' is the Reynolds number, 'a' is the air-gap length, 'R_r' is the rotor radius,'ρ' is the air density, 'v' is the air velocity, 'μ' is the dynamic viscosity of air, 'D_e' is the hydraulic diameter,'λ' is the thermal conductivity of the air, and 'Pr' is air Prandtl number. An alternative methodology of analyzing the air flow in the airgap is presented in [25, 26], where an equivalent effective conductivity is applied, considering both laminar flow and turbulent flow. With the above conditions, the derived heat transfer coefficient is around 274.9 W/(m^2·K).

Heat transfer coefficient in the water jacket depends on the cooling channel design and the water flow velocity (10L/min in this case) in the channel. It can be calculated with formulae (11) to (14) when the flow is turbulent [24], where 'f' is the friction factor, 'Re' is the Reynolds number, 'Pr' is the coolant Prandtl number, 'D_h' is the hydraulic diameter, 'v' is the water velocity, 'μ' is the dynamic viscosity of water, while 'S' and 'P' are the cross sectional area and peripheral length of the water channel respectively. With water thermal conductivity 'λ', formula (14)

is used to calculate the heat transfer coefficient between the coolant and housing, which is about 986 W/(m^2·K).

$$Nu = \frac{(f/8)\times(Re-1000)\times Pr}{\left[1+12.7\times(f/8)^{1/2}\times\left(Pr^{2/3}-1\right)\right]} \quad (11)$$

$$f = (0.79 \times ln(Re) - 1.64)^{-2} \quad (12)$$

$$D_h = 4S/P\,;\ \mathrm{Re} = \rho v D_h/\mu \quad (13)$$

$$h = \lambda \mathrm{Nu}/D_h; \quad (14)$$

C. Thermal results

From the foregoing discussion, the selection of slot number is a sensitive multidomain problem as on one side, by increasing the slot number, the thermal path for heat dissipation is shortened, while on the other side, the copper and iron losses can increase markedly, due to the discussed effects of fill factor, winding factor and armature reaction field. The thermal benefit, if any, is therefore determined by the optimal balance between the aforesaid parameters.

The currents and associated losses corresponding to the same output torque for each machine variant, as shown in Fig. 6, and Fig. 8 are applied to the thermal model described in the previous section II.B. The thermal network solves when a defined convergence is achieved, where thermal conductivities (and losses) are adjusted with the winding temperature. Fig. 10 shows the calculated temperatures for the same output torque.

The reduced thermal resistance is in a largely dominant role over the increased losses for all the investigated motors (24-slot, 36-slot and 84-slot), with peak winding temperature monitored decreasing in comparison to the original motor. For the cases with the slot number 24 and 36, peak winding temperature reductions of up to -25.6 °C (-14.18%) and -32.5°C (-17.97%) are observed. For higher slot numbers (84 slots), the increase in losses starts to be in a dominant role, with the peak winding temperature being +7.7 °C (+4.23%) higher compared to the 36 slot motor, while it still provides a -24.8°C (-13.73%) peak winding temperature reduction with respect to the original 12-slot motor.

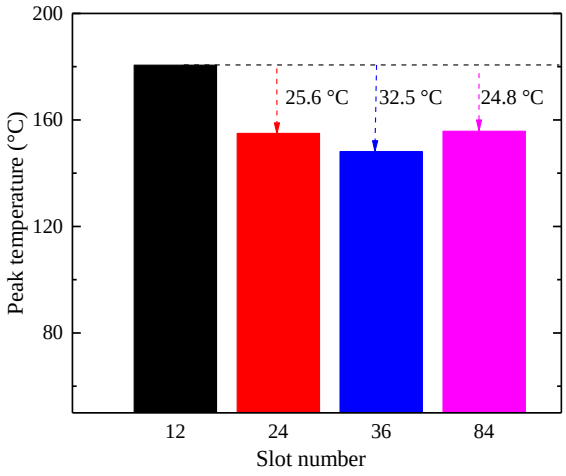

Fig. 10. Peak temperatures of motors with different slot number for the same output torque

D. Electromagnetic performance with different slot number

Considering the thermo-electromagnetic multi-disciplinary design aspects and factors in play as the slot number is optimized, Fig. 11 shows the calculated extra continuous torque entitlement for the same peak winding temperature (i.e. 180 °C). For the aforesaid thermal limit of the original 12-slot motor, significant torque improvements are observed in the cases with slot number being 24 and 36, corresponding to 4.24Nm(+4.74%) and 5.73Nm(+6.45%), respectively. The 84-slot motor also translates to 3.99Nm (+4.45%) increase in torque with respect to the original motor, while it is 1.74Nm(-1.86%) less compared to the 36-slot motor.

Apart from the discussed thermo-electromagnetic aspects of this paper related to slot number selection, in the final design of a stator, mechanical aspects should be checked, particularly on the stator teeth strength and their vibration as the slot number is increased. These should be carefully considered taking into account the forces exerted on the teeth, including those exerted in operation as well as during coil-insertion.

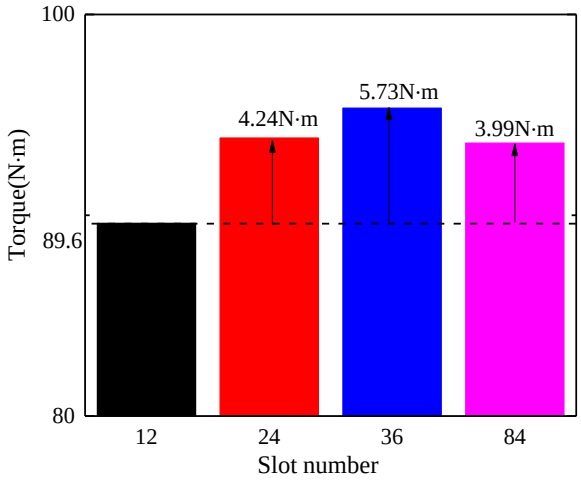

Fig. 11. Additional torque entitlement for the same winding temperature rise

E. Guidelines on optimized slot number for the investigated marine electrical machine

The thermal benefits for stators having a slot number of 12, 24, 36 and 84 were investigated in the preceding sections, suggesting that increasing the slot number can bring significant thermal benefits with respect to the original motor, while the temperature reduction is not always guaranteed by simply increasing further the slot number. This section gives a more comprehensive view of the peak temperature tendency with slot number, together with the copper fill factor and copper losses, considering all the integral slot per pole per phase '*q*' numbers, from *q*=1 to *q*=7 (i.e. 12,24,36,48,60,72,84 slots), as shown in Fig. 12.

Peak temperature tendency with slot number depends on the balance between the extra losses incurred and the shortened thermal path, as shown in Fig. 12 (a). It decreases, reaching a minimum when the slot number is 48 (*q*=4), and then increases with higher slot numbers. It is worth noting that peak temperature reduction is especially sensitive for low slot

numbers (i.e. when increasing the slot number from 12 to 24).

From Fig. 12 (b), it can be seen that the copper fill factor decreases linearly with the slot number due to the extra slot liner area added, while copper losses are increasing at a varying rate. Copper losses increase with the slot number because of: (i) current increase due to the reduced winding factor, with the losses increasing with the square of the current, and (ii) increased resistance from the reduced copper fill and in some cases (when the slot number is over 60) from the increasing winding temperature. In increasing the slot number from 12 to 24, there is a big increase in current to maintain the same output torque, and thus copper losses increase significantly. On the other hand, copper losses are increasing rapidly due to the combined effects of increasing winding temperature and reduced copper fill for slot numbers over 60. For slot numbers between 36 and 60, copper losses increase linearly with slot number. In this slot number range, both the winding temperature variation, as well as the current variation are less pronounced.

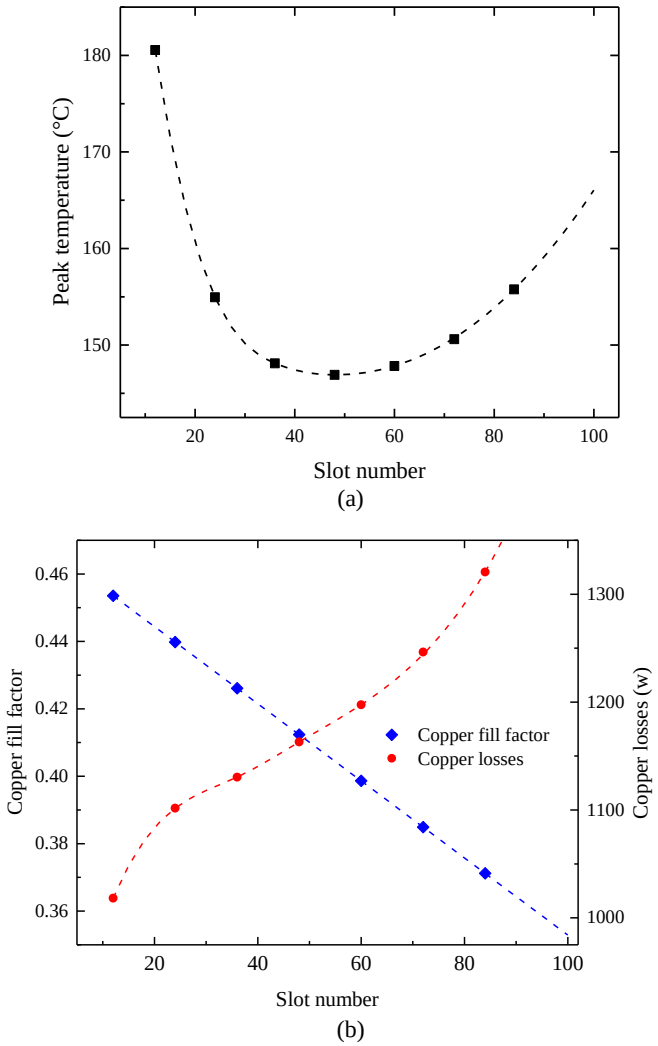

Fig. 12. a) Peak temperature versus slot number b) Copper fill factor and copper losses variation with slot number

F. Guidelines on optimized slot number for temperature reduction

The previous sections have described the considerations and methodology to arrive at the optimized slot number from a thermal perspective for the investigated 42kW 4-pole marine generator. Using a similar analysis methodology, this study is extended to generate guidelines on optimized slot number selection considering a series of scaled machines. It is assumed that both the ratio of slot width to tooth width and the ratio of rotor outer diameter to stator outer diameter remain the same, giving reliable guideline values for machines of a similar pole number to the case study investigated. In this case, 0.4 to 4 times the dimensions of the original 42kW machine are considered, with the stator outer diameter varying from 98mm to 1000 mm. Based on the aforesaid analysis, the optimized slot number for temperature minimization is plotted versus the stator outer diameter in Fig. 13. From this figure, it can be seen that optimized slot number increases linearly with the stator dimension when the stator outer diameter is from 98mm to 400mm and starts to flatten out with further increase of stator diameter. It is worth mentioning that it is expected that the thermally optimized slot number indicated in Fig. 13 may not always be practical from an electromagnetic design point of view, in which case an appropriately close slot number value following the trend line in the figure can be chosen.

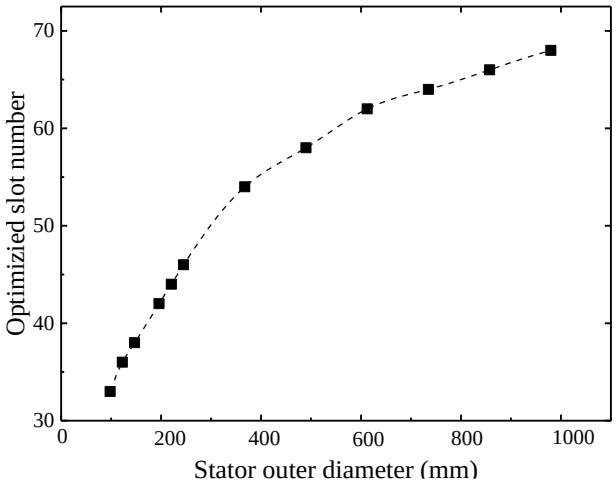

Fig. 13. Optimized slot number from thermal perspective

Following the same methodology and procedure carried out for determining the optimum slot number for the 42kW machine, a detailed design of a 4-pole 1MW surface-PM machine is performed, and the machine built as shown in Fig. 14. The key electrical and geometrical parameters are listed in Table 2, with the stator OD of 600mm being an order of magnitude larger than that of the earlier case study.

Fig. 14. 1MW 4-pole, 60-slot SPM machine stator

TABLE 2

PARAMETERS FOR A 4-POLE 1MW SURFACE-PM GENERATOR

	Parameters	Values
Machine rating	Rated power	1MW
	Rated speed	3000rpm
Geometry	Stator outer diameter	600mm
	Active length	650mm
Materials	Insulation	C class

The same phenomenon of Fig. 12(a) recurs in Fig. 15(a) for the 1MW machine, where for lower slot numbers (in this case <48 slots), as the slot number is increased the peak temperature reduces sharply, with the temperature increasing again for the higher slot numbers. Considering the larger stator diameter of 600mm, the optimum slot number for reducing the winding temperature in this case is 60 slots (i.e. 5 slots per pole per phase), which also concurs to the value indicated from the earlier study corresponding to Fig. 13.

Fig. 15 (b) shows the trend of the copper fill factor and copper losses for the 1MW machine case study. The copper fill factor, as in the previous case, has a linearly decreasing relationship with slot number, albeit the rate of decrease (gradient) is less due to the larger total slot area of the 1MW machine.

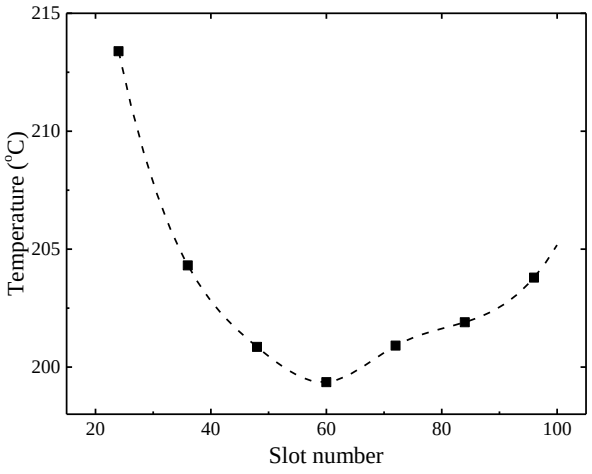

(a)

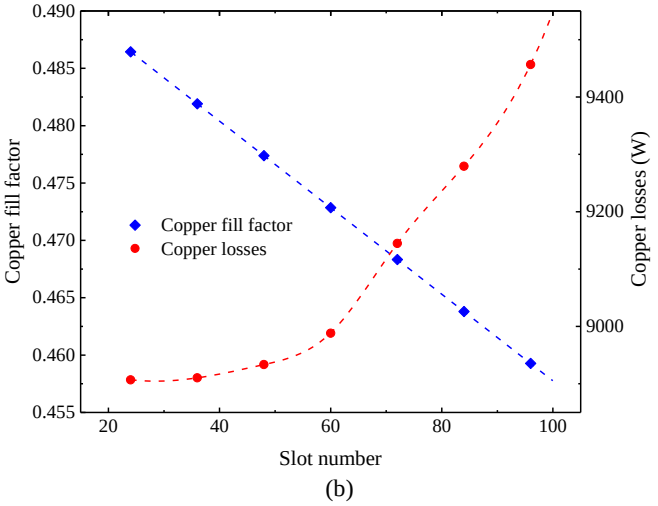

(b)

Fig. 15. 1MW machine (a) Peak temperature versus slot number (b) Copper fill factor and copper losses variation with slot number

III. EXPERIMENTAL VALIDATION

A. *Test segments and experimental rig*

Three segments based on the original 12-slot stator, as well as the presented 24-slot and 36-slot stators are described and tested in this section to validate the analysis on optimized slot number of section II. For the sake of keeping the experimental setup simple, quarter-sectors of the whole stator and a specially designed water jacket are manufactured . The axial length of the segments is the same as with the original motor. Since the main losses investigated in this research are the copper losses in the slot and their thermal path, the segments are made of solid steel to simplify the manufacturing process, and tests performed using DC currents. In this section the segments are referred to as: original segment A (q=1), double-slot segment B (q=2) and triple-slot segment C (q=3), shown in Fig. 16.

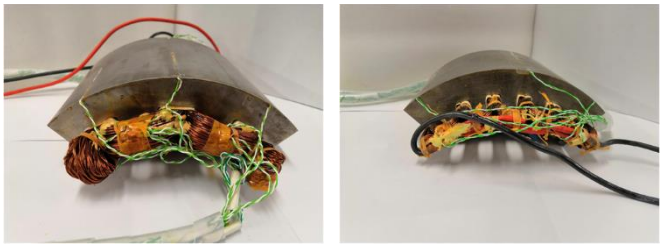

(a) (b)

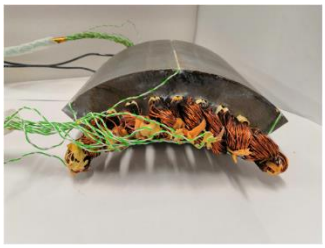

(c)

Fig. 16. Segments for experimental validation, (a)Segment A; (b) Segment B; (c) Segment C.

The number of wires per turn are adjusted based on the slot number and copper fill factor for each segment, corresponding to that shown in Fig. 2. Multiple thermocouples (K-type) are placed in the slots to give a clear indication of the hot spot within the segments, as shown in Fig. 17 (each ● representing a thermocouple), including one in the middle of each slot where the hotspot within the segment is expected based on thermal modelling. Also thermocouples are inserted in the middle of the end-winding to measure the hot spot of the end-winding. Thermocouples are also fixed to the segments' back-iron with thermal paste as can be easily spotted from Fig. 16. These are used to detect and ensure good contact between the segments and the cooling water jacket. Segments are then varnished using vacuum pressure impregnation (VPI), which ensures consistency and a good fill quality by the impregnation resin inside the slot.

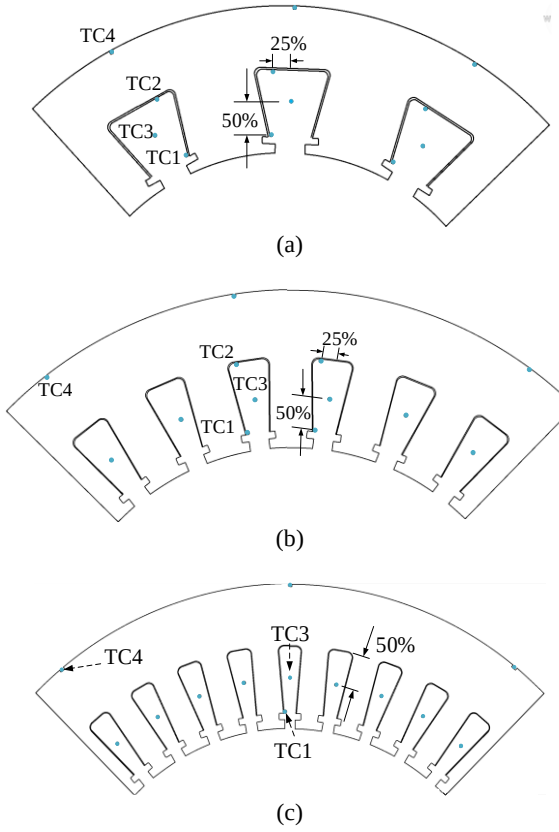

Fig. 17. Thermocouple locations, (a)Segment A; (b) Segment B; (c) Segment C.

The segments are fed by a DC current and completely insulated from air, so that all the losses generated are removed to the water-jacket. The experimental assembly is shown in Fig. 18, detailing the various constituent parts.

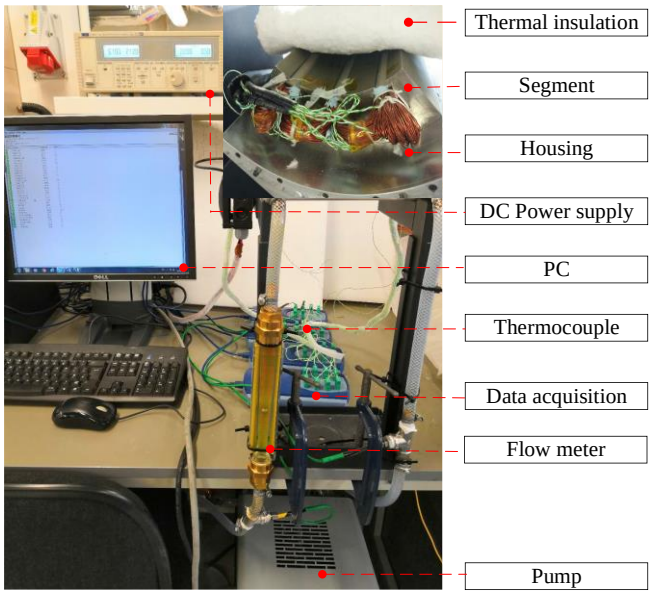

Fig. 18. Experimental rig

B. Test segments' thermal model

The LPTN thermal model developed for the full machine in section II has been validated with short circuit tests and is adjusted to simulate the segment tests with practical modifications made, mainly removing the rotor. The thermal condition that no heat loss is dissipated to the ambient from the end-windings and the inner surface of the stator core is assumed, since the segments are covered by a thermal insulation layer during the experiments, as detailed in Fig. 18. Also, since only DC current is applied to the coil, no heat is generated in the stator core (i.e. no iron losses within the test segment). All the heat generated inside the copper is conducted through the stator core, water jacket and then removed by water flowing through the water jacket. Therefore, in the thermal network simulations for the segment, the convective heat transfer in the air-gap and at the end-winding are neglected. The winding loss distribution in the segment is equivalent to that in the design process of the full machine, calculated based on the input currents and the electrical resistance of the winding. Meanwhile, the scaling losses of winding temperature are considered. The thermal model was calibrated with the highest temperature the winding can tolerate, which is 180 °C in this case. Other input currents are also used to gauge the overall effectiveness of the thermal model.

C. Experimental results

To ease the comparison, only peak winding temperatures are used herewith, the experimental data of which is summarized and shown in Fig. 19 for all three test segments. As seen from Fig. 19, the peak winding temperature of segment A is much higher than that of segment B and C when the same current is applied. For example an input current of 30.4A corresponds to a temperature of 180°C for the hotspot in segment A, while for segment B and segment C, the peak temperatures with the same input current are 136.5°C(24.2% lower) and 130.5°C(27.5%

lower), respectively.

Alternatively, for the same winding thermal limit of 180°C the current density of 8.87 A/mm^2 (corresponding to 30.4A) for the original segment, can be increased to 11.71 A/mm^2 (+32%) for segment B, and further to 13.33 A/mm^2, (+50.3%) for the segment C.

Also from Fig. 19, for all three test segments the peak winding temperature increases with the current as more heat is generated. However, the rate of increase varies for different segments. The peak winding temperature of segment A increases faster than that in segment B and segment C.

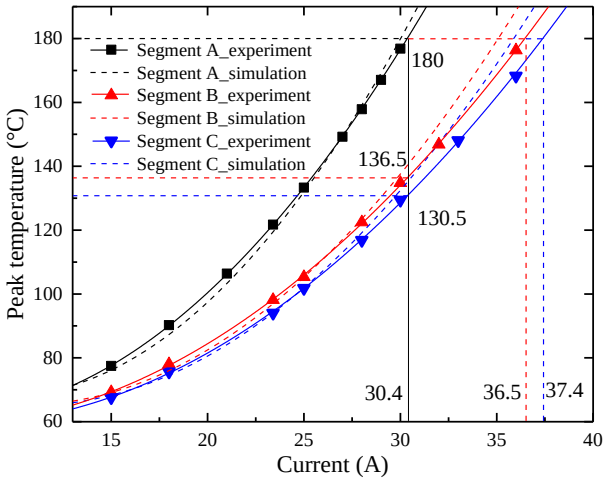

Fig. 19. Improved segments thermal benefits

D. Effects of slot number with water jacket cooling

Fig. 12 (a) presented the slot number thermal effects on the peak winding temperature for the actual machine, with the currents increased with slot number in order to maintain the same nominal machine output torque. This characteristic is presented again in Fig. 20, in red (-Δ-). Fig. 20 also plots, in blue (-○-), the thermal effects of slot number when the same current is applied to the full machine model, while excluding the iron losses, analogous to the situation with experimental testing. On the same plot, in black (■), the experimentally measured peak winding temperature of the three test segments for the same injected current is shown. Similar to the LPTN thermal network predictions, in the experiments when the slot number increases from 12 to 24, there is a sharp reduction of the peak winding temperature. A further increasing of slot number from 24 to 36 reduces the peak temperature further albeit at a decreasing rate. This tendency also agrees well with the simulation results.

The simplified LPTN thermal model predicts well the thermal performances of the segments for all the tested experimental cases. Due to the limitation of manufacturing and winding technologies available to the authors, test segments with higher slot numbers (>48 slots) were not practical to be prototyped for the motor size investigated. Therefore, the validated LPTN model is used to predict the cooling performance with the further increasing of slot number. From Fig. 20, it is shown the benefit of any further slot number increasing will be quite limited for 48-slots (q=4), and detrimental for 60 slots or higher (q≥5). It should be pointed out that similar analysis methodology and further experiments on electrical machines with, for example, larger geometries, are suggested to the readers in order to identify and validate the optimal slot number for each case in hand.

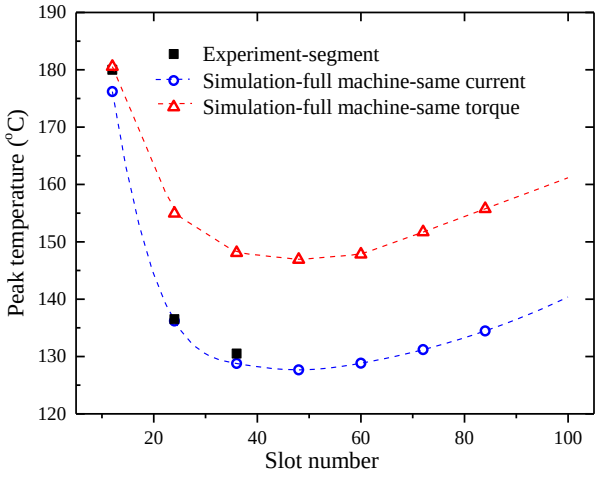

Fig. 20. Peak temperature versus slot number for different scenarios

IV. Conclusion

To increase the market uptake of electrical machines for more-electric transportation, a step change in performance metrics is required. The winding copper losses are often the bottleneck in improving the performance metrics, being it the power density or cost performance, due to the low effective thermal conductivity in the slot. Often improvements to tackle this come at the cost of using more expensive materials or more intensive cooling arrangements. While these are of course effective, in this paper it has been shown that prior to resorting to such techniques, it is important to pay careful attention to the more basic design choices from the thermal perspective, such as the slot number which is shown to be a particularly sensitive thermo-electrical optimisation parameter. Taking an existing 42kW, 4-pole 12-slot electrical machine, and using a methodological multi-domain approach which takes into account the various factors that need consideration, this paper has shown experimentally that the current density can be increased by over 50% by optimizing the slot number. Such increase is quite significant, particularly in light of the performance entitlement it can translate to. Furthermore, adopting the analysis methodology presented in this paper, guidelines are given on slot number selection for temperature reduction for a range of stator diameters, which should be a useful reference for the initial motor design stages.

V. References

[1] D. Golovanov, L. Papini, D. Gerada, Z. Xu, and C. Gerada, "Multidomain Optimization of High-Power-Density PM Electrical Machines for System Architecture Selection," *IEEE Transactions on Industrial Electronics*, vol. 65, no. 7, pp. 5302-5312, 2018.

[2] D. Gerada, X. Huang, C. Zhang, H. Zhang, X. Zhang, and C. Gerada, "Electrical machines for automotive electrically assisted turbocharging," *IEEE/ASME Transactions on Mechatronics*, vol. 23, no. 5, pp. 2054-2065, 2018.

[3] D. Gerada, Z. Xu, X. Huang, and C. Gerada, "Fully-integrated high-speed IM for improving high-power marine engines," *IET Electric Power Applications*, vol. 13, no. 2, pp. 148-153, 2019, doi: 10.1049/iet-epa.2018.5328.
[4] M. Galea, C. Gerada, T. Raminosoa, and P. Wheeler, "A thermal improvement technique for the phase windings of electrical machines," *IEEE Transactions on Industry Applications*, vol. 48, no. 1, pp. 79-87, 2012.
[5] J. Zhang, Z. Zhang, Y. Xia, and L. Yu, "Thermal Analysis and Management for Doubly Salient Brushless DC Generator With Flat Wire Winding," *IEEE Transactions on Energy Conversion*, vol. 35, no. 2, pp. 1110-1119, 2020, doi: 10.1109/TEC.2020.2966046.
[6] M. Liu, Y. Li, H. Ding, and B. Sarlioglu, "Thermal management and cooling of windings in electrical machines for electric vehicle and traction application," in *Transportation Electrification Conference and Expo (ITEC), 2017 IEEE*, 2017: IEEE, pp. 668-673.
[7] B. Zhang, R. Qu, X. Fan, and J. Wang, "Thermal and mechanical optimization of water jacket of permanent magnet synchronous machines for EV application," in *Electric Machines & Drives Conference (IEMDC), 2015 IEEE International*, 2015: IEEE, pp. 1329-1335.
[8] Z. Xu, M. Galea, C. Tighe, T. Hamiti, C. Gerada, and S. Pickering, "Mechanical and thermal management design of a motor for an aircraft wheel actuator," in *Electrical Machines and Systems (ICEMS), 2014 17th International Conference on*, 2014: IEEE, pp. 3268-3273.
[9] C. Tighe, C. Gerada, and S. Pickering, "Assessment of cooling methods for increased power density in electrical machines," in *2016 XXII International Conference on Electrical Machines (ICEM)*, 4-7 Sept. 2016 2016, pp. 2626-2632, doi: 10.1109/ICELMACH.2016.7732892.
[10] S. Nategh, A. Krings, O. Wallmark, and M. Leksell, "Evaluation of impregnation materials for thermal management of liquid-cooled electric machines," *IEEE Transactions on Industrial Electronics*, vol. 61, no. 11, pp. 5956-5965, 2014.
[11] F. Zhang *et al.*, "Back-Iron Extension Thermal Benefits for Electrical Machines With Concentrated Windings," *IEEE Transactions on Industrial Electronics*, vol. 67, no. 3, pp. 1728-1738, 2020, doi: 10.1109/TIE.2019.2903758.
[12] M. Schiefer and M. Doppelbauer, "Indirect slot cooling for high-power-density machines with concentrated winding," in *2015 IEEE International Electric Machines & Drives Conference (IEMDC)*, 10-13 May 2015 2015, pp. 1820-1825, doi: 10.1109/IEMDC.2015.7409311.
[13] S. A. Semidey and J. R. Mayor, "Experimentation of an Electric Machine Technology Demonstrator Incorporating Direct Winding Heat Exchangers," *IEEE Trans. Industrial Electronics*, vol. 61, no. 10, pp. 5771-5778, 2014.
[14] R. Wrobel, S. J. Williamson, N. Simpson, S. Ayat, J. Yon, and P. H. Mellor, "Impact of slot shape on loss and thermal behaviour of open-slot modular stator windings," in *Energy Conversion Congress and Exposition (ECCE), 2015 IEEE*, 2015: IEEE, pp. 4433-4440.
[15] R. Wrobel, S. Ayat, and J. Godbehere, "A systematic experimental approach in deriving stator-winding heat transfer," in *2017 IEEE International Electric Machines and Drives Conference (IEMDC)*, 21-24 May 2017 2017, pp. 1-8, doi: 10.1109/IEMDC.2017.8001871.
[16] J. Godbehere, R. Wrobel, D. Drury, and P. H. Mellor, "Experimentally Calibrated Thermal Stator Modeling of AC Machines for Short-Duty Transient Operation," *IEEE Transactions on Industry Applications*, vol. 53, no. 4, pp. 3457-3466, 2017, doi: 10.1109/TIA.2017.2686328.
[17] H. Vansompel and P. Sergeant, "Extended End-Winding Cooling Insert for High Power Density Electric Machines With Concentrated Windings," *IEEE Transactions on Energy Conversion*, vol. 35, no. 2, pp. 948-955, 2020, doi: 10.1109/TEC.2019.2953577.
[18] J. Pyrhonen, T. Jokinen, and V. Hrabovcová, *Design of rotating electrical machines*. John Wiley & Sons, 2009.
[19] G. Bertotti, "General properties of power losses in soft ferromagnetic materials," *IEEE Transactions on magnetics*, vol. 24, no. 1, pp. 621-630, 1988.
[20] D. M. Ionel, M. Popescu, M. I. McGilp, T. Miller, S. J. Dellinger, and R. J. Heideman, "Computation of core losses in electrical machines using improved models for laminated steel," *IEEE Transactions on Industry Applications*, vol. 43, no. 6, pp. 1554-1564, 2007.
[21] C. Mejuto, M. Mueller, D. Staton, S. Mebarki, and N. Al-Khayat, "Thermal Modelling of TEFC Alternators," in *IECON 2006 - 32nd Annual Conference on IEEE Industrial Electronics*, 6-10 Nov. 2006 2006, pp. 4813-4818, doi: 10.1109/IECON.2006.347908.
[22] A. Boglietti, A. Cavagnino, D. Staton, M. Shanel, M. Mueller, and C. Mejuto, "Evolution and modern approaches for thermal analysis of electrical machines," *IEEE Transactions on industrial electronics*, vol. 56, no. 3, pp. 871-882, 2009.
[23] D. Staton, A. Boglietti, and A. Cavagnino, "Solving the more difficult aspects of electric motor thermal analysis in small and medium size industrial induction motors," *IEEE Transactions on Energy Conversion*, vol. 20, no. 3, pp. 620-628, 2005.
[24] V. Gnielinski, "New equations for heat and mass transfer in turbulent pipe and channel flow," *Int. Chem. Eng.*, vol. 16, no. 2, pp. 359-368, 1976.
[25] W. Li, X. Zhang, S. Cheng, and J. Cao, "Thermal optimization for a HSPMG used for distributed generation systems," *IEEE Transactions on Industrial Electronics*, vol. 60, no. 2, pp. 474-482, 2013.
[26] V. Hatziathanassiou, J. Xypteras, and G. Archontoulakis, "Electrical-thermal coupled calculation of an asynchronous machine," *Archiv für Elektrotechnik*, vol. 77, no. 2, pp. 117-122, 1994.

Fengyu Zhang received B.E degree in thermal engineering from Huazhong University of Science and Technology, Wuhan, China in 2014 and Ph.D. degree in electrical machines from University of Nottingham in 2019. She is currently a Research Fellow in the area of thermal management on electrical machines within the PEMC group at University of Nottingham. Her main research interests include high performance motors for transport applications and their multi-domain optimization.

David Gerada received the Ph.D. degree in high-speed electrical machines from University of Nottingham, Nottingham, U.K., in 2012.

From 2007 to 2016, he was with the R&D Department at Cummins, Stamford, U.K., first as an Electromagnetic Design Engineer (2007– 2012), and then as a Senior Electromagnetic Design Engineer and Innovation Leader (2012– 2016). At Cummins, he pioneered the design and development of high-speed electrical machines, transforming a challenging technology into a reliable one suitable for the transportation market, while establishing industry-wide-used metrics for such machinery. In 2016, he joined the University of Nottingham where he is currently a Principal Research Fellow, responsible for developing state-of-the-art electrical machines for future transportation which push existing technology boundaries, while propelling the new technologies to higher technology readiness levels.

Dr. Gerada is a Chartered Engineer in the U.K. and a member of the Institution of Engineering and Technology.

Zeyuan Xu received the Ph.D. degree in mechanical engineering from the University of Manchester, Manchester, U.K., in 2002.

He subsequently worked as a Research Fellow at UMIST, Brunel University, and University of Nottingham. He is currently a Senior Research Fellow in thermo-mechanical design of high speed electrical machines within the PEMC group at University of Nottingham, Nottingham, U.K. His main research interests include turbulent thermo-fluid flow, heat transfer enhancement, and thermal management of advanced electrical machines and power electronics.

Xiaochen Zhang(S'09-M'12) graduated from Harbin University of Science and Technology and received Master's Degree in 2006. He graduated from Harbin Institute of Electrical Technology and received Doctor's Degree in 2012.

He is with the Department of Electric and Electronic Engineering, University of Nottingham Ningbo China. His research interests include research on electromagnetic and thermal analysis on electrical machine, especially in permanent magnetic machines and high speed machines.

Chris Tighe received the MEng and Ph.D. degrees in mechanical engineering from the University of Nottingham, U.K., in 2007 and 2011, respectively. After graduating, he spent time working in the electrical generator industry and in various research and commercial machine development positions at the University of Nottingham. He is now the proprietor of Electrical Cooling Solutions, an engineering design consultancy specialising in the thermal management of electrical machines and power electronics.

He Zhang received his B.Eng. degree from Zhejiang University, China, in 2002. He obtained the MSc. and Ph.D. degree in electrical machines from The University of Nottingham, UK, in 2004 and 2009 respectively. After this he worked as Research Fellow at the University and Director of BestMotion Technology Centre. He moved to University of Nottingham Ningbo China as Senior Research Fellow in 2014, promoted to Principal Research Fellow in 2016 and to Professor in 2020.

Currently he is the Director of Nottingham Electrification Centre (NEC) within the Power electronics, Machines and Control research group in University Of Nottingham. His research interests include high performance electric machines and drives for transport electrification.

Wei Hua (SM'16) received the B.Sc. and Ph.D. degrees in electrical engineering from Southeast University, Nanjing, China, in 2001 and 2007, respectively. From 2004 to 2005, he was with the Department of Electronics and Electrical Engineering, The University of Sheffield, U.K., as a Joint-Supervised Ph.D. Student. Since 2007, he has been with Southeast University, where he is currently a Chief Professor of Southeast University and a Distinguished Professor of Jiangsu Province. He has co-authored over 150 technical papers. He holds 50 patents in his areas of interest. His teaching and research interests include design, analysis, and control of electrical machines, especially for PM brushless machines and switching reluctance machines, etc.

Chris Gerada (SM'12) is an Associate Pro-Vice-Chancellor for Industrial Strategy and Impact and Professor of Electrical Machines. His principal research interest lies in electromagnetic energy conversion in electrical machines and drives, focusing mainly on transport electrification. He has secured over £20M of funding through major industrial, European and UK grants and authored more than 350 referred publications. He received the Ph.D. degree in numerical modelling of electrical machines from The University of Nottingham, Nottingham, U.K., in 2005. He subsequently worked as a Researcher with The University of Nottingham on high-performance electrical drives and on the design and modelling of electromagnetic actuators for aerospace applications. In 2008, he was appointed as a Lecturer in electrical machines; in 2011, as an Associate Professor; and in 2013, as a Professor at The University of Nottingham. He was awarded a Research Chair from the Royal Academy of Engineering in 2013. Prof. Gerada served as an Associate Editor for the IEEE TRANSACTIONS ON INDUSTRY APPLICATIONS and is the past Chair of the IEEE IES Electrical Machines Committee.